

# A novel therapeutic target for peripheral nerve injury-related diseases: aminoacyl-tRNA synthetases

Byung Sun Park<sup>1</sup>, Seung Geun Yeo<sup>2</sup>, Junyang Jung<sup>1,\*</sup>, Na Young Jeong<sup>3,\*</sup>

1 Department of Anatomy and Neurobiology, School of Medicine, Kyung Hee University, Seoul, Republic of Korea

2 Department of Otolaryngology, Head and Neck Surgery, School of Medicine, Kyung Hee University, Seoul, Republic of Korea

3 Department of Anatomy and Cell Biology, College of Medicine, Dong-A University, Busan, Republic of Korea

## Abstract

Aminoacyl-tRNA synthetases (AminoARSs) are essential enzymes that perform the first step of protein synthesis. Beyond their original roles, AminoARSs possess non-canonical functions, such as cell cycle regulation and signal transduction. Therefore, AminoARSs represent a powerful pharmaceutical target if their non-canonical functions can be controlled. Using AminoARSs-specific primers, we screened mRNA expression in the spinal cord dorsal horn of rats with peripheral nerve injury created by sciatic nerve axotomy. Of 20 AminoARSs, we found that phenylalanyl-tRNA synthetase beta chain (FARSB), isoleucyl-tRNA synthetase (IARS) and methionyl-tRNA synthetase (MARS) mRNA expression was increased in spinal dorsal horn neurons on the injured side, but not in glial cells. These findings suggest the possibility that FARSB, IARS and MARS, as a neurotransmitter, may transfer abnormal sensory signals after peripheral nerve damage and become a new target for drug treatment.

**Key Words:** nerve regeneration; aminoacyl-tRNA synthetases; dorsal horn; peripheral nerve injury; *in situ* hybridization; neural regeneration

**Funding:** This study was supported by Basic Science Research Program through the National Research Foundation of Korea (NRF) funded by the Ministry of Science, ICT and Future Planning (2015R1A2A2A01002735 to JJ; 2015R1C1A1A02036863 to NYJ).

Park BS, Yeo SG, Jung J, Jeong NY (2015) A novel therapeutic target for peripheral nerve injury-related diseases: aminoacyl-tRNA synthetases. *Neural Regen Res* 10(10):1656-1662.

## \*Correspondence to:

Junyang Jung, M.D., Ph.D. or

Na Young Jeong, M.D., Ph.D.,

jjjung@khu.ac.kr or jnyjy@dau.ac.kr

## orcid:

0000-0003-3946-5406 (Junyang Jung)

0000-0002-7922-9793 (Na Young Jeong)

doi: 10.4103/1673-5374.167766

http://www.nrronline.org/

Accepted: 2015-08-12

## Introduction

Aminoacyl-tRNA synthetases (AminoARSs) are essential enzymes involved in ligation of specific amino acids to their cognate tRNAs. These enzymes charge tRNA in three cellular locations: the nucleus, cytoplasm and mitochondria (Lund and Dahlberg, 1998; Bonnefond et al., 2005; Lodish et al., 2007). Thus, AminoARSs are ubiquitously expressed in living cells and are involved in basic cellular functions, such as protein synthesis and cell viability. There are two classes of AminoARSs: Groups I and II. A Rossmann nucleotide-binding fold in Group I AminoARSs alternates with  $\beta$ -strands and  $\alpha$ -helices in their active sites, whereas Groups II AminoARSs contain a seven-stranded  $\beta$ -sheet with flanking  $\alpha$ -helices (Arnez and Moras, 1997). Both Groups I and II share the same core structure, contrary to the structure of their catalytic domains (Arnez and Moras, 1997).

In addition to translation, a canonical AminoARS function, a large number of studies have demonstrated non-canonical roles of AminoARSs, including cell cycle regulation and signal transduction. Secreted human glycyl-tRNA synthetase (GARS) and lysyl-tRNA synthetase (KARS) are implicated in defense against tumorigenesis and in triggering the proinflammatory response (Park et al., 2005b, 2012). Tyrosyl-tRNA synthetase (YARS) and tryptophanyl-tRNA

synthetase (WARS) act as angiogenic cytokines on endothelial cells after secretion into the extracellular space (Wakasugi and Schimmel, 1999; Wakasugi et al., 2002a, b; Tsuda et al., 2005). Increasing evidence points to novel non-canonical AminoARS functions.

In the nervous system, AminoARS dysfunction causes neuronal diseases. Inherited peripheral neuropathies [e.g., Charcot-Marie-Tooth disease type 2D and dominant intermediate CMT (DI-CMT)] are caused by heritable mutations in GARS and YARS, respectively (Antonellis et al., 2003; Jordanova et al., 2006). Specifically, distribution defects are observed in GARS mutants, both in *in vitro* and in *in vivo* neuronal cells, suggesting a disease-causing factor (Nangle et al., 2007; Seo et al., 2014). In addition, amyotrophic lateral sclerosis, a motor neuron disease caused by a mutation in Cu/Zn superoxide dismutase 1 (SOD1), is also likely to be linked to abnormal AminoARS function. In transgenic mouse models, SOD1 G85R and G93A mutations are selectively lethal to motor neurons (Kunst et al., 1997). In an animal model, SOD1 mutations had a novel interaction with KARS that was not observed with wild-type SOD1 (Kunst et al., 1997). These previous studies indicate that abnormal AminoARS function in neuronal cells induces nervous system disorders. After peripheral nerve injury, AminoARS

expression patterns were changed in dorsal root ganglion (DRG). KARS and glutamyl-tRNA synthetase (QARS) mRNA was decreased in the neurons of dorsal root ganglion (DRG), but not in satellite cells, after peripheral nerve injury (Park et al., 2015). These results indicate that AminoARSs may play a role of signaling molecules in sensory neurons.

This study aimed to assess the expression profiles of AminoARSs in the spinal cord dorsal horn following peripheral nerve injury.

## Materials and Methods

### Animals

Animal experiments were performed in male adult Wistar rats, weighing 200–250 g. Rats were housed with free access to food and water in a temperature- and humidity-controlled ( $23 \pm 1^\circ\text{C}$ ; 50%) environment on a 12-hour light/dark cycle, and cages were changed weekly. All animal procedures were performed in accordance with standard guidelines for animal experiments determined by Kyung Hee University Institutional Animal Care and Use Committee (KHUASP [SE]-13-027). All efforts were made to minimize the number of animals used and the suffering of the animals.

### Tissue processing

After anesthesia by an intraperitoneal injection of pentobarbital sodium (50 mg/kg), rat's left sciatic nerve was axotomized at the mid-thigh level. Seven days after axotomy, L<sub>4-6</sub> spinal cord segments were collected and stored under appropriate conditions for later experiments. For immunohistochemistry, spinal cord tissue was perfused with 4% paraformaldehyde in 0.1 M phosphate buffer and then cut into 16  $\mu\text{m}$  thick sections using a cryostat (Leica, Wetzlar, Germany). For reverse transcription-polymerase chain reaction (RT-PCR) and western blot analysis, L<sub>4-6</sub> segments of the spinal cords were quickly immersed into liquid nitrogen.

### Semi-quantitative RT-PCR

RT-PCR analysis was performed on the tissue described above. In brief, RNA was isolated from the spinal cord and then reverse transcribed with oligo dT using SuperScript<sup>®</sup> III (Invitrogen Corporation, Carlsbad, CA, USA). RT-PCR was performed using specific primers for AminoARS. The designed primers and each of the acronyms are described in **Table 1**. RT-PCR was performed using several PCR cycles depending on the target genes (**Table 1**), with an annealing temperature of  $60^\circ\text{C}$ . Products were separated on an agarose gel and visualized using GelRed<sup>™</sup> (Biotium, Hayward, CA, USA). The total mRNA level was normalized to the GAPDH mRNA level. To examine changes in AminoARS mRNA levels after peripheral nerve injury, we designed a total of 20 PCR primers and amplified the rat AminoARSs. PCR of cDNA reverse transcribed from total RNA was performed in the spinal cord. Of the 20 AminoARSs examined by semi-quantitative RT-PCR, phenylalanyl-tRNA synthetase beta chain (FARSB), isoleucyl-tRNA synthetase (IARS) and MARS expression was altered in the spinal dorsal horn after peripheral nerve injury.

### In situ hybridization

Rat cDNA fragments for AminoARSs were amplified by RT-PCR, and subcloned into the pGEM<sup>®</sup>-T Easy Vector (Promega, Madison, WI, USA). Plasmids were linearized, and digoxigenin-labeled cRNA probes were prepared by *in vitro* transcription using T7 RNA Polymerase (Promega) and SP6 RNA Polymerase (Promega). All pre-hybridization procedures were conducted in RNase-free conditions at room temperature. Section slides were dried, fixed in 4% paraformaldehyde in 0.1 M phosphate buffer for 20 minutes at room temperature. After three rinses in phosphate-buffered saline (PBS) for 15 minutes each with 0.1% active diethyl pyrocarbonate (DEPC), slides were equilibrated in  $5\times$  saline sodium citrate (SSC) for 15 minutes at room temperature. After the equilibration process, the slides were pre-hybridized in 50% formamide,  $5\times$  SSC and 40  $\mu\text{g}/\text{mL}$  salmon sperm DNA for 2 hours at room temperature. Hybridization was performed overnight at  $55^\circ\text{C}$  with 400 ng/mL of digoxigenin-labeled probe in 50% formamide,  $5\times$  SSC and 40  $\mu\text{g}/\text{mL}$  salmon sperm DNA. Hybridized sections were rinsed in  $2\times$  SSC for 30 minutes at room temperature, washed in  $2\times$  SSC for 2 hours at  $65^\circ\text{C}$  and subsequently in  $0.1\times$  SSC at  $65^\circ\text{C}$ . After rinsing, the sections were equilibrated in Buffer 1 (100 mM Tris-HCl, 150 mM NaCl, pH 7.5) for 5 minutes. They were then incubated in Buffer 2 (Buffer 1 containing 0.3% blocking reagent; Roche, Mannheim, Germany) with 1:5,000 diluted alkaline phosphatase (AP)-coupled anti-digoxigenin antibody (Roche) for 2 hours at room temperature. After two 15-minute rinses in Buffer 1, the sections were equilibrated in Buffer 3 (100 mM Tris-HCl, 100 mM NaCl, 50 mM MgCl<sub>2</sub>, pH 9.5). Sections were then stained overnight in Buffer 3 containing 200- $\mu\text{L}$  nitro-blue tetrazolium and 5-bromo-4-chloro-3'-indolyphosphate (NBT/BCIP) mix (Roche) per 10 mL of Buffer 3. The slides were then washed with PBS and mounted. The *in situ* hybridization samples were detected and analyzed using a microscope (Axioskop2; Carl Zeiss, Oberkochen, Germany).

### Immunohistochemistry

Before staining, slides were fixed in 4% paraformaldehyde for 10 minutes. After three washes in PBS, the samples were permeabilized in PBS containing 0.3% Triton X-100 (Biosesang, Sungnam, Korea) (PBST) and blocked with 5% bovine serum albumin (BSA; Biosesang) and 5% fetal bovine serum (FBS; Hyclone, Logan, UT, USA) overnight at  $4^\circ\text{C}$ . Mouse anti-neuronal nuclear antigen (NeuN; 1:1,000; Millipore, Billerica, MA, USA), rabbit anti-ionized calcium-binding adapter molecule 1 (Iba-1; 1:500; Wako Chemicals, Richmond, VA, USA), goat anti-gial fibrillary acidic protein (GFAP; 1:500; Santa Cruz Biotechnology, Santa Cruz, CA, USA) and mouse anti-2'3'-cyclic-nucleotide 3'-phosphodiesterase (CNPase; 1:500; Sigma, St. Louis, MO, USA) primary antibodies were placed on the slides, which were incubated for 1 hour at room temperature. After three washes with PBS, slides were incubated for 2 hours at room temperature with Alexa Fluor<sup>®</sup> 488 or 594 (1:1,000; Invitrogen, Carlsbad, CA, USA) secondary antibodies. The slides were then washed three times in PBS and mounted. Immunofluorescence was detected and analyzed

using a laser scanning confocal microscope (LSM700; Carl Zeiss, Oberkochen, Germany).

### Western blot analysis

Spinal dorsal horn (L<sub>4-5</sub>) tissue samples were homogenized in modified radioimmunoprecipitation assay buffer [RIPA; 50 mM Tris-HCl (pH 7.4), 150 mM NaCl, 0.5% deoxycholic acid, 0.5% Triton X-100, 1 mM phenylmethylsulfonyl fluoride, 1 mM sodium o-vanadate, 1× protease inhibitor cocktail tablet (Roche Molecular Biochemicals, Nutley, NJ, USA)]. After centrifugation for 30 minutes at 4°C, the supernatant was used for western blot analysis.

Western blot analysis was performed according to a previous study (Seo et al., 2014). We used the following primary antibodies: a polyclonal rabbit anti-FARSB (1:200; Proteintech, Chicago, IL, USA), a polyclonal rabbit anti-IARS (1:200; Neomics, Seoul, Korea), a polyclonal rabbit anti-MARS (Neomics, 1:200), a polyclonal rabbit anti-TARS (1:200; Gentex, San Antonio, TX, USA) and a monoclonal antibody against β-actin (1:5,000; Sigma). For quantification, images were scanned and analyzed with the LAS image analysis system (Fujifilm, Tokyo, Japan). Optical density (band intensity) ratios of FARSB, IARS, MARS and TARS to β-actin were calculated.

### Statistical analysis

Data (differences between groups) are expressed as the mean ± SD and were statistically analyzed using SPSS software (IBM, Armonk, New York, USA). Student's *t*-test was used. A *P* value of < 0.001 was considered statistically significant.

## Results

### Changes of FARSB, IARS and MARS mRNA and protein expression

Seven days after sciatic nerve injury, FARSB, IARS and MARS mRNA expression was significantly increased in the injured L<sub>4-5</sub> spinal cord compared with the control L<sub>4-5</sub> regions (Figure 1A). The 17 remaining AminoARSs had similar mRNA expression patterns in both control and injured samples (data not shown). Semi-quantitative analysis of relative AminoARS intensities also showed increased FARSB, IARS and MARS mRNA expression in the injured spinal cord compared with the control side (Figure 1B). Next, we performed the time course analysis to investigate the pattern changing of FARSB, IARS and MARS expression at control, 1, 3 and 7 days using RT-PCR. The expression of FARSB, IARS and MARS in the dorsal horn on day 1 after nerve injury was significantly increased and their increases were maintained until 7 days after nerve injury (Figure 1C and D).

To investigate the protein expression of FARSB, IARS and MARS, we performed western blot analysis. Predominant FARSB, IARS and MARS bands were observed from tissue harvested from injured spinal dorsal horn combined with control side (Figures 2A). After nerve injury, the fold increases of FARSB, IARS and MARS in the injured dorsal horn were  $3.32 \pm 0.25$ ,  $2.25 \pm 0.17$  and  $2.83 \pm 0.16$ , respectively (Figure 2B). However, TARS, as a negative control, did

not show any fold change ( $1.05 \pm 0.11$ ) in the optical density (band intensity) in western blot analysis.

To confirm these changes in animal tissues and to further identify the cell types expressing AminoARSs, *in situ* hybridization and immunohistochemistry were performed using DIG-labeled probes and antibodies. First, we assessed AminoARS expression in the spinal dorsal horn using *in situ* hybridization. Eight total probes were used for *in situ* hybridization: AARS, CARS, FARSB, IARS, KARS, LARS, MARS and TARS. Similar to RT-PCR data and western blot analysis (Figures 1, 2), FARSB, IARS and MARS expression was significantly increased on the injured side compared to control side (Figure 3A). Quantitative analysis of relative FARSB, IARS and MARS optical density (Figure 3B) revealed increased FARSB, IARS and MARS mRNA expression on the injured side compared to the control side. In addition, *in situ* hybridization revealed that AARS, CARS, KARS, LARS and TARS mRNA was expressed at similar levels on both the injured and control sides (Supplementary Figure 1 online).

### Increases in FARSB, IARS and MARS mRNA expression

Local identification of the increased FARSB, IARS and MARS mRNA in the spinal cord tissue is very important to predict their functions in the injured spinal dorsal horn. In other words, the increased FARSB, IARS and MARS mRNA could be characterized according to the cell types in which they are localized, for example, as neurotransmitters, cytokines, and chemokines. Thus, to confirm the cell types that expressed FARSB, IARS and MARS, we immunostained *in situ* hybridization samples with anti-NeuN, anti-GFAP, anti-Iba-1 and anti-CNPase antibodies as markers of neuronal cell bodies, astrocytes, microglia and oligodendrocytes, respectively. In *in situ* hybridization using FARSB probes, digoxigenin-positive signals were increased on the injured side and were co-localized with NeuN, but not glial fibrillary acidic protein (GFAP), Iba-1 or CNPase (Figure 4A and Supplementary Figure 2 online). We also observed increased IARS and MARS mRNA expression on the injured side, and their digoxigenin-positive signals were co-localized with NeuN, but not GFAP, Iba-1 or CNPase (Figure 4A and Supplementary Figure 2 online). These findings indicate that expression of FARSB, IARS and MARS mRNA was increased in neuronal cell bodies of the spinal dorsal horn. FARSB, IARS and MARS mRNA expression was increased in neuronal cell bodies, and to a lesser extent in astrocytes, microglia, and oligodendrocytes (Figure 4B).

## Discussion

Previous studies showed that AminoARSs have several non-canonical functions, which involve a large number of molecular events in living cells (Park et al., 2005a; Son et al., 2014). Many studies reported that AminoARSs are related to nervous system disorders, such as Charcot-Marie-Tooth disease, amyotrophic lateral sclerosis and encephalopathy (Kunst et al., 1997; Antonellis et al., 2003; Jordanova et al., 2006; Scheper et al., 2007). In addition, peripheral sensory neurons showed the decrease of KARS and QARS mRNA expression after nerve injury (Park et al., 2015). These alterations of KARS and QARS mRNA may indicate that KARS

**Table 1 Primer sequences and product sizes of aminoARSs**

Gene symbol	AminoARSs	Primer	Sequence (5'-3')	Product size and PCR condition	GenBank ID
AARS	Ethionyl-tRNA synthetase	F R	ACA TGG CCT ACA GGG TTC TG ATC TAC CAC CAG GCC CTT CT	436 bp 92°C 30 sec, 55°C 30 sec, 72°C 30 sec, 30 cycles	NM_001100517.1
CARS	Cysteinyl-tRNA synthetase	F R	TGT GAA GCT TGC CAC AGA A TTG GGA GAG CGT TTC TCA CT	479 bp 92°C 30 sec, 55°C 30 sec, 72°C 30 sec, 30 cycles	NM_001106319.1
DARS	Aspartyl-tRNA synthetase	F R	CGG CGG AAG ATT ATG CTA A CTC TCC CGT CCT CTT CTC CT	456 bp 92°C 30 sec, 55°C 30 sec, 72°C 30 sec, 30 cycles	NM_053799.2
EPRS	Glutamyl-prolyl-tRNA synthetase	F R	AAT CCT GCG CTA CTT GGC T TGC ATG CCC AAT GTG TAA GT	487 bp 92°C 30 sec, 55°C 30 sec, 72°C 30 sec, 30 cycles	NM_001024238.1
FARSA	Phenylalanyl-tRNA synthetase alpha subunit	F R	GAT AAT CCC GTC TTG GAG CA ATC ACT TCG GTC AGC AGC TT	501 bp 92°C 30 sec, 55°C 30 sec, 72°C 30 sec, 30 cycles	NM_001024237.1
FARSB	Phenylalanyl-tRNA synthetase beta subunit	F R	GAC AGC AAT GGA GTG GTC CT GTC CTC CAC AAT GTC ACA CG	429 bp 92°C 30 sec, 55°C 30 sec, 72°C 30 sec, 30 cycles	NM_001004252.1
GARS	Glycyl-tRNA synthetase	F R	ATC GGA AGC TCT GAC TCG AA AAG CAG CCA CTG AGG AAA AA	426 bp 92°C 30 sec, 55°C 30 sec, 72°C 30 sec, 25 cycles	NM_001271139.1
HARS	Histidyl-tRNA synthetase	F R	TGT CAT CAA GCT CCG TTC AG TTT TTA GCG GCA GAG ACG TT	493 bp 92°C 30 sec, 55°C 30 sec, 72°C 30 sec, 30 cycles	NM_001025414.1
IARS	Isoleucyl-tRNA synthetase	F R	TCA TTG CGT TCT TTG AGA CG CAA GAG CTT CTG GGT CTT GG	473 bp 92°C 30 sec, 55°C 30 sec, 72°C 30 sec, 30 cycles	NM_001100572.1
KARS	Lysyl-tRNA synthetase	F R	CTA CCA CAA CGA GCT GGA CA TTT GCGA GTT TCT TCG GTC T	410 bp 92°C 30 sec, 55°C 30 sec, 72°C 30 sec, 30 cycles	NM_001006967.1
LARS	Leucyl-tRNA synthetase	F R	TCA GGG AAG AGT GCT GTC CT GAC TTT TCC GTT TGC ATG GT	409 bp 92°C 30 sec, 55°C 30 sec, 72°C 30 sec, 25 cycles	NM_001009637.1
MARS	Methionyl-tRNA synthetase	F R	GCT GTC AGC AAT GAA CCT GA TCT GCA GAG GAG TGG TTG TG	445 bp 92°C 30 sec, 55°C 30 sec, 72°C 30 sec, 30 cycles	NM_001127659.1
NARS	Asparaginyl-tRNA synthetase	F R	TGA CAA AGA TGC TGG AGT CG AGT ACA GCC CAT CGG AAC AC	422 bp 92°C 30 sec, 55°C 30 sec, 72°C 30 sec, 25 cycles	NM_001025635.2
QARS	Glutaminyl-tRNA synthetase	F R	GTG GTG GAG AAC GGT GAA GT CCT TTG AGC TCT TCC CCT CT	482 bp 92°C 30 sec, 55°C 30 sec, 72°C 30 sec, 30 cycles	XM_003752229.2
RARS	Arginyl-tRNA synthetase	F R	TAT GAG CCG CCT CTT TGA GT AGG CAC GAA CAC AAT TTT CC	442 bp 92°C 30 sec, 55°C 30 sec, 72°C 30 sec, 30 cycles	NM_001105777.2
SARS	Seryl-tRNA synthetase	F R	CCG TGA GTT GGT TTC CTG TT CTC TCT GTT CCA GGG CAG AC	445 bp 92°C 30 sec, 55°C 30 sec, 72°C 30 sec, 25 cycles	NM_001007606.1
TARS	Threonyl-tRNA synthetase	F R	TTT GTC TCT CAG CGG TCC TT TTG GAG GGC CGT AAC ATA AG	474 bp 92°C 30 sec, 55°C 30 sec, 72°C 30 sec, 33 cycles	NM_001006976.1
VARS	Valyl-tRNA synthetase	F R	GGA CAA CAT CCG AGA CTG GT TGA CAT TGC CGA GAG ACT TG	474 bp 92°C 30 sec, 55°C 30 sec, 72°C 30 sec, 33 cycles	NM_053292.1
WARS	Tryptophanyl-tRNA synthetase	F R	AAG TGA CAC CGT GGA GGA AC TCC ATC TGA CCA CAC GAC AT	482 bp 92°C 30 sec, 55°C 30 sec, 72°C 30 sec, 30 cycles	NM_001013170.2
YARS	Tyrosyl-tRNA synthetase	F R	TAC CAA AGG CAC CGA CTA CC AGG AAA GAG GAC GTG CTT GA	460 bp 92°C 30 sec, 55°C 30 sec, 72°C 30 sec, 30 cycles	NM_001025696.1
GAPDH	Glyceraldehyde-3-phosphate dehydrogenase	F R	CTA CAT GGT CTA CAT GTT CCA GTA TG AGT TGT CAT GGA TGA CCT TGG	380 bp 92°C 30 sec, 55°C 30 sec, 72°C 30 sec, 30 cycles	NM_008084

AminoARSs: Aminoacyl-tRNA synthetases; sec: seconds.

and QARS serve as neurotransmitters to transfer abnormal sensory signals to spinal cord dorsal horn because some AminoARSs are secreted to extracellular space (Wakasugi and Schimmel, 1999; Wakasugi et al., 2002a, b; Park et al., 2005b, 2012; Tsuda et al., 2005). Therefore, we performed AminoARS mRNA expression screening in spinal dorsal horn under the assumption that the spinal dorsal horn may show altered AminoARS expression after peripheral nerve injury.

We screened for 20 rat AminoARS genes using semi-quantitative RT-PCR and compared gene expression between control and injured spinal dorsal horn. We found increased

expression of FARSB, IARS and MARS on the ipsilateral side, evaluated the morphological pattern of AminoARS expression, and determined AminoARS-expressing cell types using *in situ* hybridization. After peripheral injury, FARSB, IARS and MARS mRNA expression was increased in neuronal cell bodies of the injured dorsal horn (**Figure 4A and B**).

After peripheral injury, FARSB, IARS and MARS mRNA expression was increased in neuronal cell bodies of the injured dorsal horn (**Figure 4A and B**). Peripheral nerve injury amplifies sensory transfer to increase synaptic transmission from sensory neurons to spinal dorsal horn neurons (Woolf

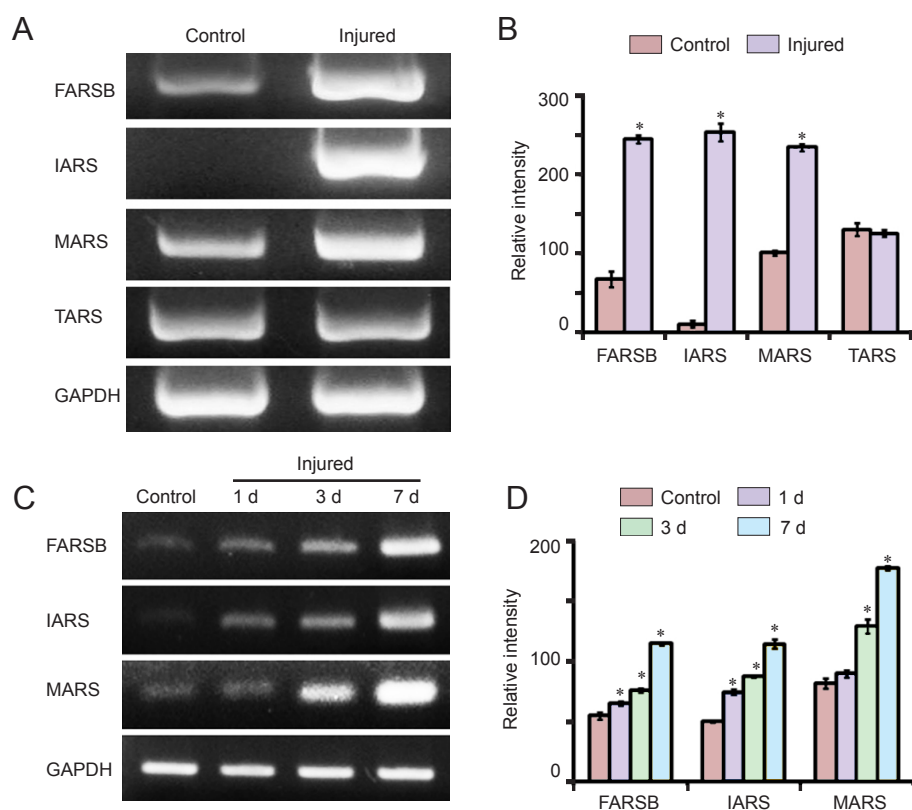


**Figure 1 Aminoacyl-tRNA synthetases (AminoARSs) mRNA expression in the spinal dorsal horn.**

(A) RNA (5 µg), extracted from rat spinal dorsal horn, was analyzed by reverse transcription-polymerase chain reaction. Phenylalanyl-tRNA synthetase beta chain (FARSB), isoleucyl-tRNA synthetase (IARS) and methionyl-tRNA synthetase (MARS) mRNA expression was increased in the injured spinal dorsal horn. Control: An uninjured animal. Glyceraldehyde 3-phosphate dehydrogenase (GAPDH) was used as a loading control. (B) Semi-quantification of the relative intensity of FARSB, IARS, MARS and threonyl-tRNA synthetase (TARS) mRNA levels in the spinal dorsal horn. Bar represents the mean ± SD. \* $P < 0.001$ , vs. control ( $n = 6$ ; Student's *t*-test). (C) Time course of FARSB, IARS and MARS mRNA expression in the L<sub>4-5</sub> spinal dorsal horn at control, days 1, 3 and 7 after nerve injury. (D) Semi-quantitative analysis reveals increased FARSB, IARS and MARS mRNA expression, measured as relative optical density ratios of FARSB, IARS and MARS bands to GAPDH, on days 1, 3, and 7 after nerve injury. \* $P < 0.001$ , vs. control ( $n = 4$ ; Student's *t*-test). d: Day(s).

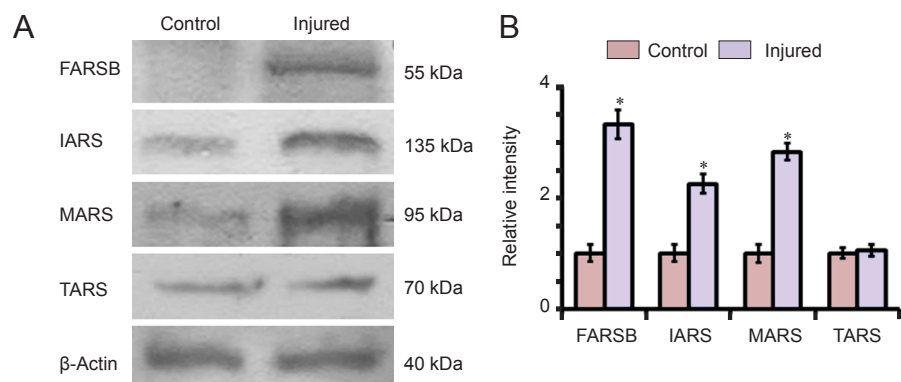


**Figure 2 FARSB, IARS and MARS protein expression in the spinal dorsal horn after sciatic nerve axotomy.**

(A) Western blot analysis of FARSB, IARS and MARS protein after axotomy. Protein extracted from control and injured spinal dorsal horn on day 7 after axotomy was subjected to western blot analysis. β-Actin was used as an internal control. (B) Quantification of FARSB, IARS and MARS protein expression levels in the L<sub>4-5</sub> spinal dorsal horn. Optical density ratios of FARSB, IARS, MARS and TARS bands to β-actin were calculated. \* $P < 0.001$ , vs. control ( $n = 5$ ; Student's *t*-test). FARSB: Phenylalanyl-tRNA synthetase beta chain; IARS: isoleucyl-tRNA synthetase; MARS: methionyl-tRNA synthetase.

and Salter, 2000; Scholz and Woolf, 2007). Signals from damaged peripheral neurons may affect the increase in FARSB, IARS and MARS expression in spinal dorsal horn neurons through synaptic transmission. Another possibility is that microglia, which is activated in the spinal dorsal horn after peripheral nerve injury (Shir et al., 2001; Tsuda et al., 2005), may act to increase FARSB, IARS and MARS expression in spinal dorsal horn neurons through indirect synaptic transmission but the interaction with microglia by a roundabout route. Because FARSB, IARS and MARS were increased in the dorsal horn at day 1 after the nerve injury (Figure 1C and D), astrocytes which are activated at around 10 days after the nerve injury (Zhuang et al., 2006) may be not involved in the increase of FARSB, IARS and MARS expression in the injured dorsal horn.

Because some AminoARSs have secretion capacity and

non-canonical functions (e.g., cell cycle regulation and signal transduction) (Wakasugi and Schimmel, 1999; Wakasugi et al., 2002a, b; Park et al., 2005b, 2012; Tsuda et al., 2005), in the dorsal horn, secondary neurons activated by signal transfer that originated from the injured primary sensory neurons or by the interaction with activated glial cells may be able to secrete FARSB, IARS and MARS, into a synaptic cleft headed for brain, to subsequently reach the brain *via* several tracts and to initiate neurobiological changes in the brain. Thus, FARSB, IARS and MARS may act as a neurotransmitter which regulates the transfer of abnormal sensory signals induced by peripheral nerve damage to the brain and this may be an instance among the many non-canonical functions of AminoARSs in the nervous system.

Additionally, in the spinal cord dorsal horn, peripheral nerve damage-induced changes in molecular events are linked

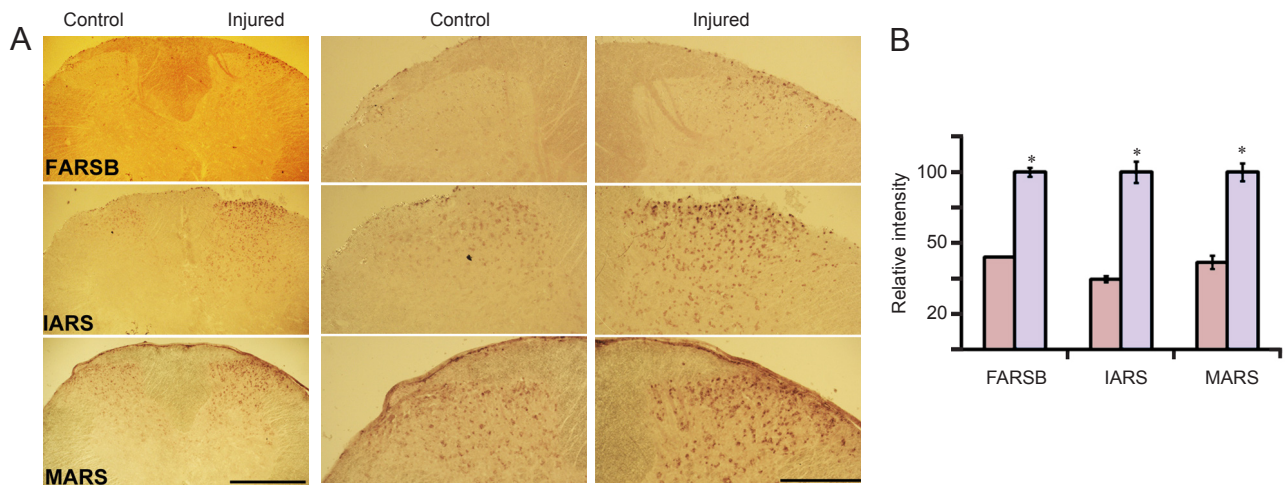


**Figure 3 Distribution of FARSB, IARS and MARS mRNA after sciatic nerve axotomy.**

(A) FARSB, IARS and MARS mRNA expression detected by DIG-labeled probes in the spinal dorsal horn on day 7 after unilateral axotomy (right side). On the injured side, FARSB, IARS and MARS hybridization signals were observed. Middle and right panels are high-magnification representations of the left panel. Scale bars: 500  $\mu\text{m}$  (left panel) and 200  $\mu\text{m}$  (middle and right panels). (B) Quantitative analysis of the relative DIG-positive intensities of FARSB, IARS and MARS mRNA levels in the spinal dorsal horn. The DIG-positive intensity was measured as the relative optical density of each band to  $\beta$ -actin (mean  $\pm$  SD) in a randomly selected area (100  $\times$  100  $\mu\text{m}^2$ ). (B) \* $P < 0.001$ , vs. control ( $n = 6$ ; Student's  $t$ -test). DIG: Digoxigenin; FARSB: Phenylalanyl-tRNA synthetase beta chain; IARS: isoleucyl-tRNA synthetase; MARS: methionyl-tRNA synthetase.

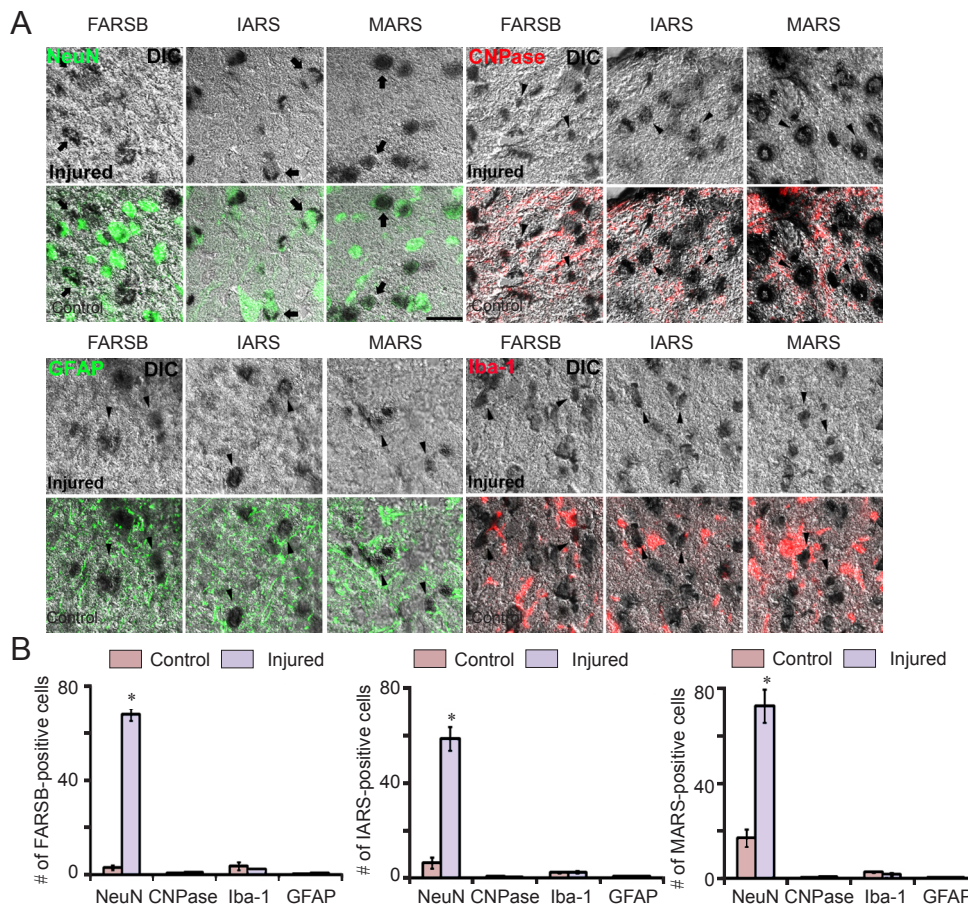


**Figure 4 In situ hybridization (ISH) demonstrating FARSB, IARS and MARS mRNA localization after sciatic nerve axotomy.**

(A) In the rat injured dorsal horn at 7 days, fluorescence immunohistochemistry was performed for neuronal nuclear antigen (NeuN, green), 2',3'-cyclic-nucleotide 3'-phosphodiesterase (CNPase, red), ionized calcium-binding adapter molecule 1 (Iba-1, red) and glial fibrillary acidic protein (GFAP, green). All FARSB, IARS and MARS mRNA-expressing cells in the spinal dorsal horn were NeuN-positive (arrows). Arrowheads indicate non-overlapping FARSB, IARS and MARS mRNA expression as shown by CNPase, Iba-1, GFAP immunoreactivities. Bar: 40  $\mu\text{m}$ . (B) Quantitative analysis of digoxigenin-positive cells in the spinal dorsal horn. The number of digoxigenin-positive cells among 100 cell marker-positive cells was measured in a randomly selected area (300  $\times$  300  $\mu\text{m}^2$ ). ImageJ program was used to analyze cell counts or stained areas. \* $P < 0.001$  ( $n = 5$ ; Student's  $t$ -test). Based on their immunohistochemical profile, FARSB, IARS and MARS mRNA-expressing cells were identified as neurons. FARSB: Phenylalanyl-tRNA synthetase beta chain; IARS: isoleucyl-tRNA synthetase; MARS: methionyl-tRNA synthetase.

to neuropathic pain. Many of the mechanisms responsible for neuropathic pain are involved in mRNA level changes in the spinal cord dorsal horn after peripheral nerve injury (Lacroix-Fralish et al., 2009). Time to maintain the neuropathic pain after the initiation of the pain is around 7 days after nerve injury and FARSB, IARS and MARS are increased in the injured spinal dorsal horn on day 7 after nerve injury. Because one of the causes of neuropathic pain is to transfer abnormal sensory signals into spinal dorsal horn after nerve injury, we suggest the possibility that FARSB, IARS and MARS, as a neurotransmitter, may transfer abnormal sensory signals after peripheral nerve damage. Thus, although we showed preliminary data for neuropathic pain, pharmacological modulation of AminoARS expression may be a useful approach for the treatment of neuropathic pain. It is, therefore, important to understand AminoARS gene expression profiles in the spinal cord dorsal horn after peripheral nerve injury. In this study, we described for the first time AminoARS mRNA and protein expression patterns and AminoARS mRNA cell type localization. Further evaluation is necessary to identify the functions of increased FARSB, IARS and MARS in dorsal horn neurons after peripheral nerve injury.

In conclusion, our data represent the first morphological and molecular characterizations of AminoARs in the spinal dorsal horn. We showed that the expression of FARSB, IARS and MARS mRNA was increased in injured dorsal horn neurons after peripheral nerve injury, but not in glial cells. To date, there is little information regarding AminoARs in the spinal dorsal horn after nerve injury. Thus, a detailed understanding of these genes could aid in understanding the nature and mechanism of abnormal sensory signal transduction to the brain after peripheral nerve damage. Because neuropathic pain is related to abnormal sensory signal transduction, regulation of FARSB, IARS and MARS expression may provide a novel therapeutic target for peripheral nerve injury-related diseases, including neuropathic pain.

**Author contributions:** JJ and NYJ designed this study, interpreted experimental results, wrote the paper, and were responsible for fundraising. BSP and SGY performed experiments. All authors approved the final version of this paper.

**Conflicts of interest:** None declared.

**Supplementary data:** Supplementary information is available at <http://www.nrronline.org>.

## References

Antonellis A, Ellsworth RE, Sambuughin N, Puls I, Abel A, Lee-Lin SQ, Jordanova A, Kremensky I, Christodoulou K, Middleton LT (2003) Glycyl tRNA synthetase mutations in Charcot-Marie-Tooth disease type 2D and distal spinal muscular atrophy type V. *Am J Hum Gene* 72:1293-1299.

Arnez JG, Moras D (1997) Structural and functional considerations of the aminoacylation reaction. *Trends Biochem Sci* 22:211-216.

Bonnefond L, Fender A, Rudinger-Thirion J, Giegé R, Florentz C, Sissler M (2005) Toward the full set of human mitochondrial aminoacyl-tRNA synthetases: characterization of AspRS and TyrRS. *Biochemistry* 44:4805-4816.

Jordanova A, Irobi J, Thomas FP, Van Dijk P, Meerschaert K, Dewil M, Dierick I, Jacobs A, De Vriendt E, Guergueltcheva V (2006) Disrupted function and axonal distribution of mutant tyrosyl-tRNA synthetase in dominant intermediate Charcot-Marie-Tooth neuropathy. *Nat Genet* 38:197-202.

Kunst CB, Mezey E, Brownstein MJ, Patterson D (1997) Mutations in SOD1 associated with amyotrophic lateral sclerosis cause novel protein interactions. *Nat Genet* 15:91-94.

Lacroix-Fralish ML, Tawfik VL, Tanga FY, Spratt KF, DeLeo JA (2009) Differential spinal cord gene expression in rodent models of radicular and neuropathic pain. *Anesthesiology* 104:1283-1292.

Lodish H, Berk A, Kaiser CA, Krieger M, Scott MP, Bretscher A, Ploegh H, Matsudaira P (2007) Matsudaira P *Molecular Cell Biology*. New York: Freeman.

Lund E, Dahlberg JE (1998) Proofreading and aminoacylation of tRNAs before export from the nucleus. *Science* 282:2082-2085.

Nangle LA, Zhang W, Xie W, Yang XL, Schimmel P (2007) Charcot-Marie-Tooth disease-associated mutant tRNA synthetases linked to altered dimer interface and neurite distribution defect. *Proc Natl Acad Sci U S A* 104:11239-11244.

Park BS, Jo HW, Jung J (2015) Expression profile of aminoacyl-tRNA synthetases in dorsal root ganglion neurons after peripheral nerve injury. *J Mol Histol* 46:115-122.

Park MC, Kang T, Jin D, Han JM, Kim SB, Park YJ, Cho K, Park YW, Guo M, He W (2012) Secreted human glycyl-tRNA synthetase implicated in defense against ERK-activated tumorigenesis. *Proc Natl Acad Sci U S A* 109:E640-647.

Park SG, Ewalt KL, Kim S (2005a) Functional expansion of aminoacyl-tRNA synthetases and their interacting factors: new perspectives on housekeepers. *Trends Biochem Sci* 30:569-574.

Park SG, Kim HJ, Min YH, Choi EC, Shin YK, Park BJ, Lee SW, Kim S (2005b) Human lysyl-tRNA synthetase is secreted to trigger proinflammatory response. *Proc Natl Acad Sci U S A* 102:6356-6361.

Scheper GC, van Der Kloek T, van Andel RJ, van Berkel CG, Sissler M, Smet J, Muravina TI, Serkov SV, Uziel G, Bugiani M (2007) Mitochondrial aspartyl-tRNA synthetase deficiency causes leukoencephalopathy with brain stem and spinal cord involvement and lactate elevation. *Nat Genet* 39:534-539.

Scholz J, Woolf CJ (2007) Can we conquer pain? *Nat Neurosci* 5:1062-1067.

Seo AJ, Shin YH, Lee SJ, Kim D, Park BS, Kim S, Choi KH, Jeong NY, Park C, Huh Y, Jang J (2014) A novel adenoviral vector-mediated mouse model of Charcot-Marie-Tooth type 2D (CMT2D). *J Mol Histol* 45:121-128.

Shir Y, Zeltser R, Vatine JJ, Carmi G, Belfer I, Zangen A, Overstreet D, Raber P, Seltzer Z (2001) Correlation of intact sensibility and neuropathic pain-related behaviors in eight inbred and outbred rat strains and selection lines. *Pain* 90:75-82.

Son SH, Park MC, Kim (2014) Extracellular activities of aminoacyl-tRNA synthetases: new mediators for cell-cell communication. *Top Curr Chem* 344:145-166.

Tsuda M, Inoue K, Salter MW (2005) Neuropathic pain and spinal microglia: a big problem from molecules in "small" glia. *Trends Neurosci* 28:101-107.

Wakasugi K, Schimmel P (1999) Two distinct cytokines released from a human aminoacyl-tRNA synthetase. *Science* 284:147-151.

Wakasugi K, Slike BM, Hood J, Ewalt KL, Cheresch DA, Schimmel P (2002a) Induction of angiogenesis by a fragment of human tyrosyl-tRNA synthetase. *J Biol Chem* 277:20124-20126.

Wakasugi K, Slike BM, Hood J, Otani A, Ewalt KL, Friedlander M, Cheresch DA, Schimmel P (2002b) A human aminoacyl-tRNA synthetase as a regulator of angiogenesis. *Proc Natl Acad Sci U S A* 99:173-177.

Woolf CJ, Salter MW (2000) Neuronal plasticity: increasing the gain in pain. *Science* 288:1765-1769.

Zhuang ZY, Wen YR, Zhang DR, Borsello T, Bonny C, Strichartz GR, Decosterd I, Ji RR (2006) A peptide c-Jun N-Terminal Kinase (JNK) inhibitor blocks mechanical allodynia after spinal nerve ligation: respective roles of JNK activation in primary sensory neurons and spinal astrocytes for neuropathic pain development and maintenance. *J Neurosci* 26:3551-3560.

Copyedited by Saijilafu S, Shah S, Li CH, Song LP, Zhao M